

Probing Anomalous Higgs Coupling through $\mu^+\mu^- \rightarrow H\gamma$

Ali Abbasabadi[†], David Bowser-Chao^{§,¶},
Duane A. Dicus^{*} and Wayne W. Repko[‡]

[†]*Department of Physical Sciences, Ferris State University, Big Rapids, Michigan 49307*

[§]*Department of Physics, University of Illinois at Chicago, Chicago, Illinois 60607;*

^{*}*Center for Particle Physics and Department of Physics, University of Texas,
Austin, Texas 78712*

[‡]*Department of Physics and Astronomy, Michigan State University,
East Lansing, Michigan 48824*

[¶]*Presented the talk.*

Abstract. The process $\mu^+\mu^- \rightarrow H\gamma$, though small compared to the resonance process, could be observable at proposed muon colliders, given expected integrated luminosities. The apparently leading diagrams occur at tree-level, and are proportional to the Higgs-muon coupling. We show, however, that the one-loop contribution is comparable to the tree-level amplitude. Furthermore, the one-loop diagrams, unlike those at tree-level, could be greatly enhanced by possible anomalous Higgs-top quark or Higgs-gauge boson couplings. For a 500 GeV unpolarized muon collider, the total cross section for $H\gamma$ associated production approaches 0.1 fb.

Recently, the possibility of using $\mu^+\mu^-$ colliders to investigate the properties of Higgs-bosons has received considerable attention [1,2]. There are significant advantages to studying Higgs-bosons with this type of collider, particularly if the mass is known from its discovery at, say, the LHC or NLC [2]. Under these circumstances, the width and branching ratios can be studied at the Higgs pole.

Resonance production, of course, is not the only channel for Higgs production at such colliders. Production in association with a photon has been considered in Ref. [3], where the leading tree-level diagrams (Fig. 1) involve radiation of the Higgs directly off the muon line, and thus are proportional the Higgs-muon coupling, which in turn (in the Standard Model) is proportional to the small but non-zero muon mass.

On the other hand, the analogous process $e^+e^- \rightarrow H\gamma$ has been studied [4], and found to have a cross-section comparable to the muon process, despite the relatively infinitesimal electron mass. In this case, it turns out that the one-loop diagrams are orders of magnitude larger than the tree-level diagrams, and in fact should

not be considered radiative corrections to the latter — the former persist even in the limit of zero electron mass. This process can be generalized to the hadronic reaction $q\bar{q} \rightarrow H\gamma$ [5], and to the rare decays $H \rightarrow f\bar{f}\gamma$, where the fermion f may be massless [6]. Turning back to the muon reaction, we shall see below that the one-loop contribution is comparable to the tree-level amplitude. Furthermore, the one-loop diagrams, unlike those at tree-level, could be greatly enhanced by possible anomalous Higgs-top quark or Higgs-gauge boson couplings.

For both the tree-level and loop-level diagrams discussed in detail below, we label the momentum and helicity of the μ^- (μ^+) in the center of mass frame, respectively, by $p = (E, |\mathbf{p}|\hat{z})$ ($\bar{p} = (E, -|\mathbf{p}|\hat{z})$) and λ ($\bar{\lambda}$), the photon momentum and scattering angle by $k = (\omega, \omega\hat{k})$ and θ , and the photon polarization vector and helicity by ϵ and $\lambda_\gamma = \pm 1$. The tree level diagrams for $\mu^+\mu^- \rightarrow H\gamma$ are shown in Fig. 1. The amplitudes, labelled by muon and photon helicities, are found to be:

$$\mathcal{M}_{\lambda\bar{\lambda}\lambda_\gamma}^{\text{tree}} = -i \frac{egm_\mu}{\sqrt{2}m_W} \left(\frac{1}{2p \cdot k} + \frac{1}{2\bar{p} \cdot k} \right) \cdot \begin{cases} \sin \theta [\lambda_\gamma(2|\mathbf{p}|^2 - E\omega) + |\mathbf{p}|\omega] & \lambda\bar{\lambda} = ++ \\ \sin \theta [\lambda_\gamma(2|\mathbf{p}|^2 - E\omega) - |\mathbf{p}|\omega] & \lambda\bar{\lambda} = -- \\ m_\mu \omega(1 + \lambda_\gamma \cos \theta) & \lambda\bar{\lambda} = +- \\ m_\mu \omega(1 - \lambda_\gamma \cos \theta) & \lambda\bar{\lambda} = -+ \end{cases}, \quad (1)$$

explicitly showing the extra suppression of the helicity flip amplitudes by a factor of m_μ relative to the non-flip amplitudes (where $\lambda = +$ denotes a μ^- helicity of $+1/2$.)

The one-loop amplitudes for $\mu^+\mu^- \rightarrow H\gamma$ receive contributions from pole diagrams involving virtual photon and Z exchange and from various box diagrams containing muons, gauge bosons and/or Goldstone bosons [4,8,7]. There are also double pole diagrams whose contribution vanishes. These are illustrated in Fig. 2. In the non-linear gauges we chose [4], the full amplitude consists of four separately gauge invariant terms: a photon pole, a Z pole, Z boxes and W boxes. These amplitudes take the form:

$$\mathcal{M}_{\text{pole}}^{\gamma,Z} = \mathcal{P}_{\gamma,Z}(s) (\delta_{\mu\nu} k \cdot (p + \bar{p}) - k_\mu (p + \bar{p})_\nu) \bar{v}(\bar{p}) \gamma_\mu (v_{\gamma,Z}^{\mathcal{P}} + a_{\gamma,Z}^{\mathcal{P}} \gamma_5) u(p) \epsilon_\nu^*, \quad (2)$$

$$\mathcal{M}_{\text{box}}^{\gamma,Z} = [\mathcal{B}_{\gamma,Z}(s, t, u) (\delta_{\mu\nu} k \cdot p - k_\mu p_\nu) + p \leftrightarrow \bar{p}] \bar{v}(\bar{p}) \gamma_\mu (v_{\gamma,Z}^{\mathcal{B}} + a_{\gamma,Z}^{\mathcal{B}} \gamma_5) u(p) \epsilon_\nu^*, \quad (3)$$

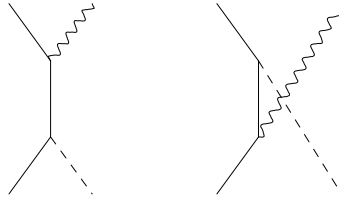


FIGURE 1. Tree level diagrams for $\mu^+\mu^- \rightarrow H\gamma$ are shown.

TABLE 1. The cross sections for the associated production of 100 GeV and 200 GeV Higgs bosons are shown together with the ratio of the signal to the square root of the background (S/\sqrt{B}) for several $\mu^+\mu^-$ collider energies. A luminosity of 100 fb^{-1} is assumed.

\sqrt{s}	$\sigma(m_H = 100 \text{ GeV})$	S/\sqrt{B}	$\sigma(m_H = 200 \text{ GeV})$	S/\sqrt{B}
500 GeV	$6.78 \times 10^{-2} \text{ fb}$	1.99	$8.76 \times 10^{-2} \text{ fb}$	3.06
1000 GeV	$2.46 \times 10^{-2} \text{ fb}$	1.50	$3.87 \times 10^{-2} \text{ fb}$	3.08
2000 GeV	$8.76 \times 10^{-3} \text{ fb}$	1.06	$1.04 \times 10^{-2} \text{ fb}$	1.72
4000 GeV	$1.54 \times 10^{-3} \text{ fb}$	0.36	$2.17 \times 10^{-3} \text{ fb}$	0.72

where $s = -(p+\bar{p})^2$, $t = -(p-k)^2$ and $u = -(\bar{p}-k)^2$. We have explicitly evaluated the form factors (\mathcal{P}_γ , etc.) in terms of the scalar functions defined in the appendices of our previous paper [4]; the results, though more complicated than those of the tree-level diagrams, are provided in Ref. [7] in closed form. In this case, as should be expected, it is the helicity *flip* contributions from the factors $\bar{v}(\bar{p})\gamma_\mu u(p)$ and $\bar{v}(\bar{p})\gamma_\mu\gamma_5 u(p)$ which survive in the $m_\mu \rightarrow 0$ limit, as can be seen, for example, by explicitly evaluating the spinor products above.

The differential cross section $d\sigma(\mu^+\mu^- \rightarrow H\gamma)/d\Omega_\gamma$ is given by

$$\frac{d\sigma(\mu^+\mu^- \rightarrow H\gamma)}{d\Omega_\gamma} = \frac{1}{256\pi^2} \frac{s - m_H^2}{\beta s^2} \sum_{\text{spin}} |\mathcal{M}^{\text{tree}} + \mathcal{M}^{\text{loop}}|^2, \quad (4)$$

with $\beta = \sqrt{1 - 4m_\mu^2/s}$. When integrating Eq. (4) to obtain the total cross section, the interference terms should be suppressed, since $\mathcal{M}_{\pm\mp}^{\text{tree}}$ and $\mathcal{M}_{\pm\pm}^{\text{loop}}$ both contain an additional factor of m_μ . This conclusion can only be invalid if the angular integration of the muon propagator factors $(1 \pm \beta \cos \theta)^{-1}$ in Eqs. (1) produces inverse powers of m_μ . This is not the case. For the $++$ or $--$ interference terms, the tree and loop amplitudes contain a factor of $\sin \theta$, which ensures that the angular integral is well behaved in the $\beta \rightarrow 1$ limit. The integral of $+-$ and $-+$ interference terms can produce a factor of β^{-1} , but this also is finite as $\beta \rightarrow 1$. As

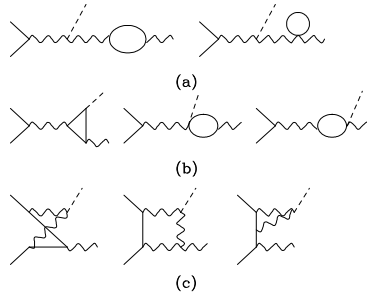


FIGURE 2. Typical diagrams for the double pole (a), single pole (b) and box (c) corrections are shown. An external solid line represents a muon, a wavy line a gauge boson, a dashed line a Higgs boson and an internal solid line a muon, gauge boson, Goldstone boson or ghost.

TABLE 2. Cross sections for the background process $\mu^+\mu^- \rightarrow \gamma b\bar{b}$ are given for several cuts on the $b\bar{b}$ invariant mass $m_{b\bar{b}}$. The last two columns are 5 GeV bins indicating, respectively, the background associated with a Higgs boson of mass 100 GeV or 200 GeV.

\sqrt{s}	$45 \text{ GeV} < m_{b\bar{b}} < \sqrt{s}$	$97.5 \text{ GeV} < m_{b\bar{b}} < 102.5 \text{ GeV}$	$197.5 \text{ GeV} < m_{b\bar{b}} < 202.5 \text{ GeV}$
500 GeV	11.1 fb	$1.16 \times 10^{-1} \text{ fb}$	$8.20 \times 10^{-2} \text{ fb}$
1000 GeV	3.80 fb	$2.69 \times 10^{-2} \text{ fb}$	$1.58 \times 10^{-2} \text{ fb}$
2000 GeV	1.21 fb	$6.83 \times 10^{-3} \text{ fb}$	$3.65 \times 10^{-3} \text{ fb}$
4000 GeV	0.37 fb	$1.81 \times 10^{-3} \text{ fb}$	$9.04 \times 10^{-4} \text{ fb}$

a consequence, we can simply add the tree [9] and one-loop cross sections to obtain $\sigma(\mu^+\mu^- \rightarrow H\gamma)$ for unpolarized muon beams. Working to leading order in m_μ , the polarized cross-sections are obtained simply by omitting the tree-level or loop-level contributions for helicity-flip or same-helicity beam polarization.

The result is illustrated in Fig. 3, where the tree, one-loop and total cross

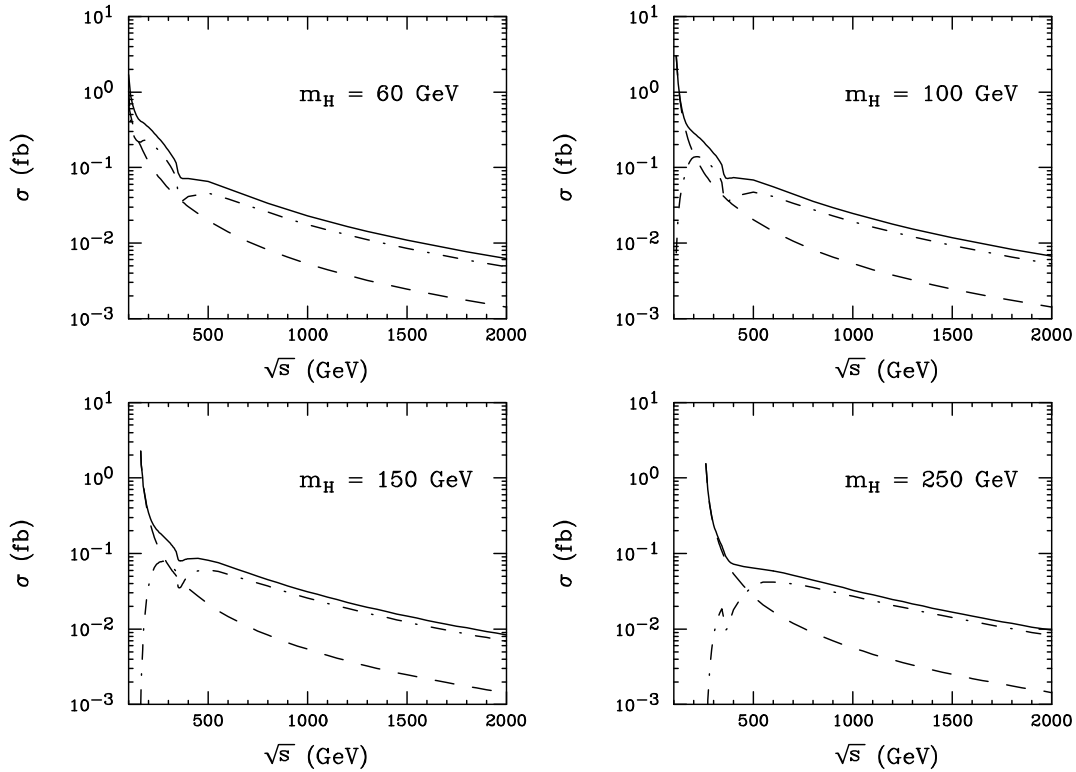


FIGURE 3. The cross section for $\mu^+\mu^- \rightarrow H\gamma$ resulting from the sum of the tree level and one-loop amplitudes is given for several values of m_H by the solid line. In each panel, the dashed line is the tree level contribution and the dot-dashed line is the one-loop contribution.

sections are plotted for several values of m_H as a function of the collider energy. For collider energies \sqrt{s} above about 500 GeV, the one-loop contribution exceeds the tree contribution. Note that Fig. 3 should not be taken literally at $\sqrt{s} \approx m_H$. As $\omega \rightarrow 0$, the tree-level process must be considered together with the virtual QED correction to the resonance process $\mu^+\mu^- \rightarrow H$ to obtain an infrared-finite $O(\alpha)$ inclusive calculation [10]. Here, we are concerned with production of the Higgs with an observable, relatively hard photon. In Table I, the total cross section is shown as a function of m_H for several collider energies. At 500 GeV, luminosities of order 100 fb^{-1} are needed to probe this channel. To make this statement more precise, we investigated the principal background $\mu^+\mu^- \rightarrow b\bar{b}\gamma$ by adapting the amplitudes for $e\bar{e} \rightarrow \mu^+\mu^-\gamma$ [11]. In Table II, the background contributions are shown for several cuts on the $b\bar{b}$ invariant mass $m_{b\bar{b}}$. In addition to these invariant mass cuts, we require the transverse momenta of the b , \bar{b} and γ to be greater than 15 GeV, their rapidities y to be less than 2.5 and the separation ΔR between the γ and the b and the γ and the \bar{b} to be greater than 0.4. The background is compared to the signal in Table I for Higgs boson masses of 100 GeV and 200 GeV. This comparison shows that, while not a discovery mode for the Higgs boson, photon-Higgs associated production can be observed with signal to square root of background ratios (S/\sqrt{B}) greater than 2 when $m_H > 100 \text{ GeV}$ at a 500 GeV collider.

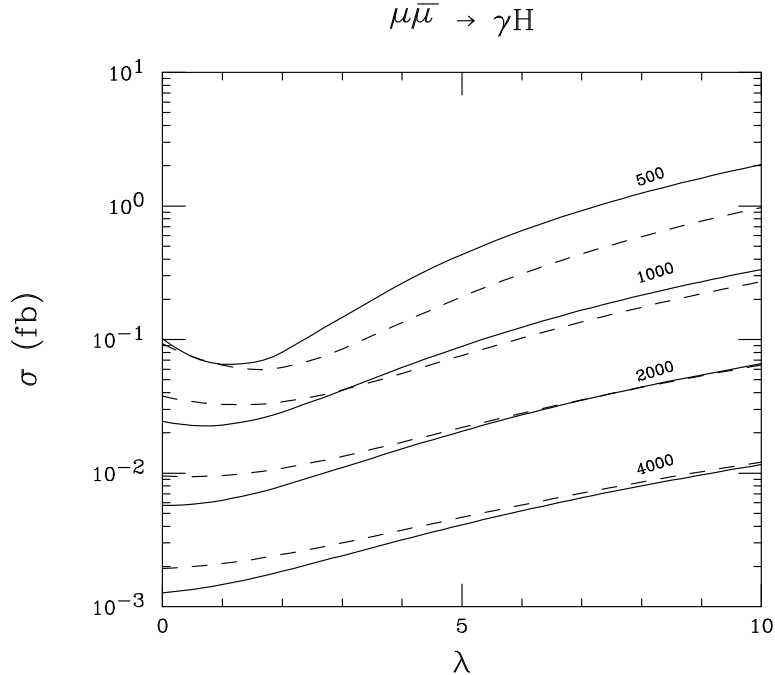


FIGURE 4. The cross section for $\mu^+\mu^- \rightarrow H\gamma$ obtained by scaling the Standard Model $t\bar{t}H$ coupling by a factor λ is shown for collider energies of 500 GeV, 1000 GeV, 2000 GeV and 4000 GeV. In each case, the solid line is $m_H = 60 \text{ GeV}$ and the dashed line is $m_H = 250 \text{ GeV}$.

Finally, we comment on how the one-loop contribution makes it possible to use $\mu^+\mu^- \rightarrow H\gamma$ as a probe of the Higgs-boson coupling to W 's, Z 's and top quarks. To provide a sense of the sensitivity of the $H\gamma$ cross section to changes in Standard Model couplings, we have varied the $t\bar{t}H$ coupling by a factor λ [12]. The result is shown in Fig. 5, where the characteristic feature is the minimum in the cross section at the Standard Model value $\lambda = 1$. For $\lambda > 1$, the cross section rises significantly. At a 500 GeV collider, observation of $H\gamma$ production with a cross section of order 1 fb would indicate some type of anomalous coupling. Anomalous Higgs-gauge boson couplings have been studied [13] for the case of $e^+e^- \rightarrow H\gamma$ where enhancement of couplings such as HZZ could result in immense enhancements to the level of 10 fb. Thus, polarization of the muon collider *opposite* to that required for optimizing resonance Higgs production may be useful in highlighting the loop-level contributions to $\mu^+\mu^- \rightarrow H\gamma$, which if unexpectedly large could signal such anomalous couplings.

This research was supported in part by the U.S. Department of Energy under Contract Nos. DE-FG013-93ER40757 and DE-FG02-84ER40173, and in part by the National Science Foundation under Grant No. PHY-93-07980.

REFERENCES

1. R. B. Palmer, A. Sessler and A. Tollestrup, *Progress on the design of a high luminosity $\mu^+\mu^-$ collider*, BNL-63245 (1996).
2. J. F. Gunion, *Muon Colliders: The Machine and The Physics*, UCD-97-17, hep-ph/9707379 (1997).
3. V. A. Litvin and F. F. Tikhonin, *Associated production of $H\gamma$ or HZ pairs at $\mu^+\mu^-$ collisions*, hep-ph/9704417 (1997).
4. A. Abbasabadi, D. Bowser-Chao, D. A. Dicus and W. W. Repko, Phys. Rev. D **52**, 3919 (1995).
5. A. Abbasabadi, D. Bowser-Chao, D. A. Dicus and W. W. Repko, hep-ph/9706335.
6. A. Abbasabadi, D. Bowser-Chao, D. A. Dicus and W. W. Repko, Phys. Rev. **D55**, 5647 (1997).
7. A. Abbasabadi, D. Bowser-Chao, D. A. Dicus and W. W. Repko, hep-ph/9708328, to appear in Phys. Rev. **D57**, (1998).
8. A. Djouadi, V. Driesen, W. Hollick and J. Rosiek, University of Karlsruhe preprint KA-TP-21-96, hep-ph/9609420.
9. The $+-$ (and $-+$) amplitudes contribute at most a few percent to the tree level cross section for $500 \text{ GeV} \leq \sqrt{s} \leq 4 \text{ TeV}$ and $60 \text{ GeV} \leq m_H \leq 300 \text{ GeV}$.
10. V. A. Litvin and F. F. Tikhonin, work in progress.
11. F. Berends *et al.*, Nucl. Phys. B **206**, 61 (1982); Z. Xu, D-H Zhang, and L. Chang, Nucl. Phys. B **291**, 392 (1987).
12. H. E. Haber, G. L. Kane and T. Sterling, Nuc. Phys. B **161**, 493 (1979).
13. G.J. Gounaris, F.M. Renard, and N.D. Vlachos, Nucl. Phys. **B459**, 51 (1996).